Performance Analysis of Distributed Radio Telescopes under Shared Spectrum Access Paradigm

Dong Han and Hlaing Minn
Department of Electrical and Computer Engineering, University of Texas at Dallas, USA
Email: dong.han6@utdallas.edu, hlaing.minn@utdallas.edu

***Abstract*—For sustainable growth and coexistence of cellular wireless communications (CWC) and radio astronomy system (RAS), a coordinated shared spectrum access paradigm was recently introduced. Embracing such paradigm, this paper proposes a distributed radio telescope (DRT) system which can geographically and spectrally coexist with CWC while offering additional capability or performance enhancement to RAS. Theoretical performance analysis of the DRT system with different quantization resolutions is presented, and approximate closed-form expressions are obtained. Furthermore, an analytical expression for the DRT system parameters under the shared spectrum access paradigm to achieve the same performance as the existing single-dish RAS with a radio quiet zone is developed to provide guidance in the DRT system design. The numerical and simulation results illustrate feasibility and potentials of the proposed DRT system.**

I. Introduction

RAS provides economically and scientifically important observations of the cosmos which benefit the society consistently [1]. As RAS signals are very weak with signal-to-noise power ratio (SNR) as low as -60 dB [2], they are highly sensitive to radio frequency interference (RFI) caused by wireless communication systems. Thus, radio telescopes are built in remote areas surrounded by radio quiet zones for interference isolation [3], [4]. However, the expansion of wireless communication systems in terms of applications, radio coverage, radio spectrum [5], and spectrum utilization [6], [7], [8] has caused increased RFI to RAS. The direct results are RFI-corrupted radio astronomical data and less radio astronomical observation opportunities and the consequence is a severe hindrance to science and knowledge discovery. On the other hand, there are increased interests and needs for expanding RAS observations, thus enlarging the conflict of spectrum access rights/needs between the two systems.

There are two types of RAS, namely single-dish telescope and telescope array. Single-dish telescope has advantages such as good potential sensitivity to large scale structure, building and maintaining simplicity and upgrading flexibility [9]. But it also has shortcomings in spatial frequency response and mechanical complexity perspectives [9] compared with the radio telescope array. A telescope array can mitigate the interference and increase the observation range and resolution. Nevertheless, these existing RAS sites are protected by radio quiet zones and cannot coexist with CWC.

This work is supported by National Science Foundation (Grant 1547048).

To mitigate the conflict between CWC and RAS, [10] and [11] recently proposed a new spectrum sharing paradigm where both systems have RFI-free guaranteed spectrum access by means of a three-phase time-division approach. [10] and [11] pointed out the instancy of embracing the new paradigm and justified that the overall spectrum utilization is enhanced by designing time-dependent durations of the spectrum access phases according to the CWC traffic statistics. Besides, the performance of CWC system under this new spectrum sharing paradigm is analyzed in [10] and [11]. An extension for coexistence of WiFi and RAS was addressed in [12].

Technical Contributions: To accommodate expansions of both CWC and RAS, we embrace the shared spectrum access paradigm of [10] and propose a DRT system which can coexist with CWC and conventional single-dish RAS. Our DRT system can either work independently as a radio telescope array or cooperate with an existing single-dish RAS to increase the overall performance accuracy. We derive analytical performance expressions for signal power estimation of the DRT system with different quantization resolutions, and then obtain approximate closed-form expressions. Next, we also obtain an analytical expression for the DRT system parameters under the shared spectrum access paradigm to achieve the same performance as the existing single-dish RAS with a radio quiet zone. This provides guidance in the DRT system design. The numerical and simulation results illustrate performance of the proposed DRT system as well as effects of ADC resolution on the RAS signal power estimation performance.

II. System Model

To enable growths in both CWC and RAS services, we consider the shared spectrum access paradigm proposed in [10] where CWC and RAS can coexist geographically and spectrally. Such coexistence paradigm removes the need of a radio quiet zone around each radio telescope and hence we propose to exploit it by introducing several radio telescopes within the radio coverage zones of CWC, which we term distributed radio telescopes (DRTs). The RAS data from each DRT are saved at a central station or a cloud database center and hence cross-processing of data from different DRTs can be easily done. This coexistence paradigm could also promote emergence of DRTs set up by public institutions, private groups or individuals with strong interest in RAS.

In the shared spectrum access approach of [10], a time frame of duration T_{f}, which consists of n_{f} subframes of

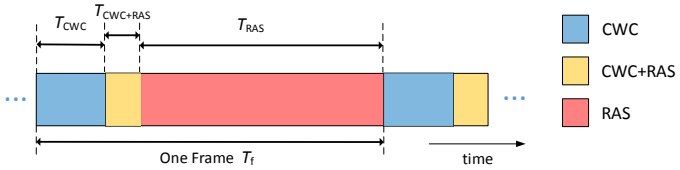

Fig. 1. Frame structure of the three-phase spectrum sharing paradigm where the durations of the phases could be different at different hours [10]

duration $T_{\rm sf}$ each, is divided into three phases, namely CWC only phase of duration $T_{\rm CWC}$ ($n_{\rm CWC}$ subframes), CWC+RAS phase of duration $T_{\rm CWC+RAS}$ ($n_{\rm CWC+RAS}$ subframes) and RAS only phase of duration $T_{\rm RAS}$ ($n_{\rm RAS}$ subframes), as is shown in Fig. 1. The first phase is only for CWC while the last phase is only for RAS, thus providing RFI-free spectrum access to both systems. The second phase is used to absorb different propagation delays of CWC cells, and it could allow transmissions in some CWC cells or some practical testing of RFI cancellation schemes. The durations of the three phases can be adjusted based on the spectrum access needs, the CWC traffic statistics, and practical fine tuning results of the shared spectrum access parameters. An example of spectrum access duration adaptation on an hourly basis based on the CWC traffic statistics was presented in [10]. For our DRT deployment, to guarantee RFI-free observation, we only use the RAS only phase for the DRT. The implication of this shared spectrum access is the reduction of the RAS observation time of a DRT if compared to the RAS in a radio quiet zone. However, more DRTs can be used to recover the loss in the RAS observation time or to get even a larger observation time. In the following, we will develop signal model, estimator, and performance analysis in a general sense based on the number of observation samples and the noise variance. By substituting appropriate values for those parameters, one can obtain the results for the the considered scenario or paradigm.

The DRT system aims to receive astronomical signals, which are commonly modeled to be zero mean complex Gaussian distributed [13]–[16], and then estimates the power of the signal. However, the received astronomical signal is significantly weaker than the additive thermal noise at the receiver. To mitigate the noise impact and achieve unbiased power estimation as accurate as possible, we apply a noise referring approach called Dicke switching (see [17, Fig.4.8] and [18]) where the receivers switch the observations between astronomical source and the inner noise generating source. Each antenna element samples and quantizes the astronomical radio signal corrupted with additive thermal noise and the reference thermal noise in a time-division manner. Next, the quantized samples are squared by the detector to obtain the signal power. Subtracting the averaged reference samples' power from the averaged noise corrupted astronomical samples' power, the power of astronomical radio signal is estimated. To be specific, for the DRT system with M antenna elements, we assume the received astronomical source signal at each antenna is circular symmetric complex Gaussian (CSCG) distributed with zero mean and variance $\sigma_{\rm s}^2$. We also assume the additive thermal noise at each antenna is distributed as zero mean CSCG with the same variance $\sigma_{\rm n}^2$. Therefore, the nth samples of the received astronomical source signal, the noise involved in astronomical observing and the referencing noise at the ith antenna are represented as $s_{\rm t}^i(n)$, $n_{\rm t}^i(n)$ and $n_{\rm r}^i(n)$, respectively, where $i \in \{1, ..., M\}$. We assume that the received signals are independent over different samples. Besides, the quantization errors at the ith antenna of the nth sample are $e_{\rm t}^i(n)$ and $e_{\rm r}^i(n)$ for astronomical observation and noise referencing, respectively. Correspondingly, the quantized samples are represented as

$$y_{\rm t}^i(n) \triangleq s_{\rm t}^i(n) + n_{\rm t}^i(n) + e_{\rm t}^i(n) \tag{1}$$

$$y_{\rm r}^i(n) \triangleq n_{\rm r}^i(n) + e_{\rm r}^i(n) \tag{2}$$

where $s_{\rm t}^i(n) \sim CN(0, \sigma_{\rm s}^2)$ and $n_{\rm t}^i(n), n_{\rm r}^i(n) \sim CN(0, \sigma_{\rm n}^2)$. Assuming we have a fixed observation time with a fixed sampling frequency, which corresponds to $2L$ samples, it can be shown that the most accurate power estimation is achieved asymptotically if we allocate L samples for astronomical observing and L samples for referencing when the following two criteria are satisfied, 1) negligible quantization error, 2) $\frac{\sigma_{\rm s}^2}{\sigma_{\rm n}^2} \to 0$. The proof is provided in Section IV. By applying this result, the output estimated source power is

$$\rho_{\rm array} = \frac{1}{ML} \sum_{i=1}^{M} \sum_{n=1}^{L} \left\{ |y_{\rm t}^i(n)|^2 - |y_{\rm r}^i(n)|^2 \right\}. \tag{3}$$

Since there is only one antenna element in single-dish system, it can be regarded as a special case of the array system. Assuming we have in total $2N$ samples and allocate N samples for astronomical observation and another N samples for noise referencing, the output estimated source power is

$$\rho_{\rm single} = \frac{1}{N} \sum_{n=1}^{N} \left\{ |y_{\rm t}(n)|^2 - |y_{\rm r}(n)|^2 \right\} \tag{4}$$

where $y_{\rm t}(n)$ and $y_{\rm r}(n)$ represent the quantized samples for astronomical observation and noise referencing of single-dish RAS, respectively.

Suppose the hourly based resource adaptation of [10] is applied and the three phases (see Fig. 1) at hour l have per-frame durations $T_{{\rm CWC},l}$ ($n_{{\rm CWC},l}$ subframes), $T_{{\rm CWC+RAS},l}$ ($n_{{\rm CWC+RAS},l}$ subframes) and $T_{{\rm RAS},l}$ ($n_{{\rm RAS},l}$ subframes), respectively, and $T_{{\rm CWC},l} + T_{{\rm CWC+RAS},l} + T_{{\rm RAS},l} = T_{\rm f}$. The total number of frames per hour is $N_{\rm f/hour} = 3600/T_{\rm f}$. Suppose the sampling frequency is $2B$ for RAS and the RAS signal power estimation is done based on K hours $\{l_k : k = 1, \cdots, K\}$. Then the number of samples available for a single DRT is $2L = 2B \sum_{k=1}^{K} T_{{\rm RAS},l_k} N_{\rm f/hour}$ while that for the conventional RAS is $2N = 2BKT_{\rm f}N_{\rm f/hour}$.

III. Performance under Finite ADC Resolutions

In this section, we analyze the mean and variance of the estimated astronomical source power for both systems. We mainly focus on the DRT system since the results are naturally applicable to the single-dish RAS by setting $M = 1$. Since the in-phase component and the quadrature-phase component of the signals are independently and identically distributed (i.i.d.), we represent the estimated power as the sum of two i.i.d. parts,

namely the in-phase estimated power $\rho_{\rm in}$ and the quadrature-phase estimated power $\rho_{\rm quad}$ where

$$\rho_{\rm in} = \frac{1}{ML}\sum_{i=1}^{M}\sum_{n=1}^{L}\left(\mathfrak{Re}\{y_{\rm t}^i(n)\}^2 - \mathfrak{Re}\{y_{\rm r}^i(n)\}^2\right) \quad (5)$$

$$\rho_{\rm quad} = \frac{1}{ML}\sum_{i=1}^{M}\sum_{n=1}^{L}\left(\mathfrak{Im}\{y_{\rm t}^i(n)\}^2 - \mathfrak{Im}\{y_{\rm r}^i(n)\}^2\right) \quad (6)$$

and $\rho_{\rm array} = \rho_{\rm in} + \rho_{\rm quad}$.

Given a b-bits quantizer with the quantization thresholds and quantized values being represented as $\tau_k,\ k \in \{1,\ldots,2^b+1\}$, and $c_k,\ k \in \{1,\ldots,2^b\}$, respectively, the second moment of the real-part quantized sample is

$$\mathbb{E}\left[\mathfrak{Re}\{y_{\rm p}^i(n)\}^2\right] = \sum_{k=1}^{2^b} c_k^2\left[Q(\tau_k/\sigma_{\rm p}) - Q(\tau_{k+1}/\sigma_{\rm p})\right] \quad (7)$$

where ${\rm p} \in \{{\rm t},{\rm r}\}$, $\sigma_{\rm t}^2 = \frac{\sigma_{\rm s}^2+\sigma_{\rm n}^2}{2}$, $\sigma_{\rm r}^2 = \frac{\sigma_{\rm n}^2}{2}$, and $Q(x) = \frac{1}{\sqrt{2\pi}}\int_x^\infty e^{-u^2/2}du$. And we have $\mathbb{E}\left[\mathfrak{Re}\{y_{\rm p}^i(n)\}^2\right] = \mathbb{E}\left[\mathfrak{Im}\{y_{\rm p}^i(n)\}^2\right]$. Define

$$\varphi_{\rm p} \triangleq \sum_{k=1}^{2^b} c_k^2\left[Q(\tau_k/\sigma_{\rm p}) - Q(\tau_{k+1}/\sigma_{\rm p})\right], \quad {\rm p} \in \{{\rm t},{\rm r}\} \quad (8)$$

$$\phi_{\rm p} \triangleq \sum_{k=1}^{2^b} c_k^4\left[Q(\tau_k/\sigma_{\rm p}) - Q(\tau_{k+1}/\sigma_{\rm p})\right], \quad {\rm p} \in \{{\rm t},{\rm r}\}. \quad (9)$$

Then, from (5)-(7), we can represent the first moment of the in-phase and quadrature-phase estimated powers as

$$\mathbb{E}[\rho_{\rm in}] = \mathbb{E}[\rho_{\rm quad}] = \varphi_{\rm t} - \varphi_{\rm r}. \quad (10)$$

We can also obtain their second moments $\mathbb{E}\left[\rho_{\rm in}^2\right] = \mathbb{E}\left[\rho_{\rm quad}^2\right]$ as in (11) shown at the top of the next page where the approximation (a) is due to the independence assumption between $y_{\rm t}^i(n)$ and $y_{\rm t}^j(n),\ \forall i \neq j$. As the power of astronomical source is significantly less than the power of noise, the approximated expression in (11) is asymptotically accurate when the received SNR approaches zero. According to (10) and (11), the variance of the in-phase estimated power and that of the quadrature-phase estimate power are

$$\mathrm{Var}(\rho_{\rm in}) = \mathrm{Var}(\rho_{\rm quad}) \approx \frac{1}{ML}(\phi_{\rm t} + \phi_{\rm r} - \varphi_{\rm t}^2 - \varphi_{\rm r}^2). \quad (12)$$

Then, we obtain the mean and variance of the power estimation of DRT system as

$$\mathbb{E}[\rho_{\rm array}] = \mathbb{E}[\rho_{\rm in}] + \mathbb{E}[\rho_{\rm quad}] = 2(\varphi_{\rm t} - \varphi_{\rm r}) \quad (13)$$

$$\begin{aligned}\mathrm{Var}(\rho_{\rm array}) &= \mathrm{Var}(\rho_{\rm in}) + \mathrm{Var}(\rho_{\rm quad}) \\ &\approx \frac{2}{ML}(\phi_{\rm t} + \phi_{\rm r} - \varphi_{\rm t}^2 - \varphi_{\rm r}^2). \end{aligned} \quad (14)$$

Next, by seting $M = 1$ and substituting L with N, we also obtain the counterparts for the single-dish RAS as

$$\mathbb{E}[\rho_{\rm single}] = 2(\varphi_{\rm t} - \varphi_{\rm r}) \quad (15)$$

$$\mathrm{Var}(\rho_{\rm single}) = \frac{2}{N}(\phi_{\rm t} + \phi_{\rm r} - \varphi_{\rm t}^2 - \varphi_{\rm r}^2). \quad (16)$$

Note that (16) is an accurate expression since for $M = 1$, (11) involves no approximation. Besides, as the effect of the noise variance is embedded in $\varphi_{\rm t}$, $\varphi_{\rm r}$, $\phi_{\rm t}$, and $\phi_{\rm r}$, a different noise variance could affect the mean and variance of the RAS power estimate. We also notice that for both the DRT system and the single-dish RAS, the mean values of the output power estimates are the same as long as they have identical quantizer settings and the same noise variance. However, the variances of the output power estimates have different factors ML versus N. This clearly shows that although $L < N$, the DRT system can improve its performance by increasing M.

IV. Approximate Closed-Form Analysis

The means and variances derived in (13) - (16) are not in closed forms. To have better insights, here, we develop approximated closed-form representations, assuming the received sample is independent of the quantization error.

For the DRT system, conditioning on the quantization errors, the received signals are regarded as being i.i.d. CSCG distributed over all the antennas, i.e.,

$$\begin{aligned} y_{\rm t}^i(n)|e_{\rm t}^i(n) &\sim CN(e_{\rm t}^i(n), \sigma_{\rm n}^2 + \sigma_{\rm s}^2) \\ y_{\rm r}^i(n)|e_{\rm r}^i(n) &\sim CN(e_{\rm r}^i(n), \sigma_{\rm n}^2). \end{aligned} \quad (17)$$

To prove the asymptotically optimal sample partitioning mentioned in Section II, we use different numbers of samples for source observation and noise referencing, namely, L_1 and L_2, and rewrite the estimated source power as

$$\rho_{\rm array} = \sum_{i=1}^{M}\sum_{n=1}^{L_1}\frac{|y_{\rm t}^i(n)|^2}{ML_1} - \sum_{i=1}^{M}\sum_{n=1}^{L_2}\frac{|y_{\rm r}^i(n)|^2}{ML_2} \quad (18)$$

where $L_1 + L_2 = 2L$. For compactness, we define $Z_{\rm t}^i \triangleq \sum_{n=1}^{L_1}|y_{\rm t}^i(n)|e_{\rm t}^i(n)|^2$ and $Z_{\rm r}^i \triangleq \sum_{n=1}^{L_2}|y_{\rm r}^i(n)|e_{\rm r}^i(n)|^2$ and note that both terms, $Z_{\rm t}^i$ and $Z_{\rm r}^i$, are non-central chi-square random variables with the means and variances being represented as

$$\mathbb{E}(Z_{\rm t}^i) = L_1(\sigma_{\rm n}^2 + \sigma_{\rm s}^2) + \sum_{n=1}^{L_1}|e_{\rm t}^i(n)|^2 \quad (19)$$

$$\mathbb{E}(Z_{\rm r}^i) = L_2\sigma_{\rm n}^2 + \sum_{n=1}^{L_2}|e_{\rm r}^i(n)|^2 \quad (20)$$

$$\mathrm{Var}(Z_{\rm t}^i) = L_1(\sigma_{\rm n}^2 + \sigma_{\rm s}^2)^2 + 2(\sigma_{\rm n}^2 + \sigma_{\rm s}^2)\sum_{n=1}^{L_1}|e_{\rm t}^i(n)|^2 \quad (21)$$

$$\mathrm{Var}(Z_{\rm r}^i) = L_2\sigma_{\rm n}^4 + 2\sigma_{\rm n}^2\sum_{n=1}^{L_2}|e_{\rm r}^i(n)|^2. \quad (22)$$

Therefore, conditioning on the quantization error set $\mathcal{E} = \{(e_{\rm t}^i(n), e_{\rm r}^i(m)) : i = 1,...,M,\ n = 1,...,L_1,\ m = 1,...,L_2\}$, the estimated power is

$$\rho_{\rm array}|\mathcal{E} = \frac{1}{ML_1}\sum_{i=1}^{M}Z_{\rm t}^i - \frac{1}{ML_2}\sum_{i=1}^{M}Z_{\rm r}^i. \quad (23)$$

From (18) to (22), the mean and variance of $\rho_{\rm array}|\mathcal{E}$ are

$$\mu_{\rho|\mathcal{E}} = \mathbb{E}[\rho_{\rm array}|\mathcal{E}] = \sigma_{\rm s}^2 + \frac{{\rm MSE_t}(L_1)}{ML_1} - \frac{{\rm MSE_r}(L_2)}{ML_2} \quad (24)$$

$$\begin{aligned}\mathrm{Var}(\rho_{\rm array}|\mathcal{E}) = &\frac{1}{ML_1}(\sigma_{\rm n}^2 + \sigma_{\rm s}^2)^2 + \frac{1}{ML_2}\sigma_{\rm n}^4 + \\ &\frac{2(\sigma_{\rm n}^2 + \sigma_{\rm s}^2)}{M^2L_1^2}{\rm MSE_t}(L_1) + \frac{2\sigma_{\rm n}^2}{M^2L_2^2}{\rm MSE_r}(L_2)\end{aligned} \quad (25)$$

where ${\rm MSE_p}(L) \triangleq \sum_{i=1}^{M}\sum_{n=1}^{L}|e_{\rm p}^i(n)|^2,\ {\rm p} \in \{{\rm t},{\rm r}\}$.

$$\mathbb{E}\left[\rho_{\text{in}}^2\right] = \frac{1}{M^2L^2}\sum_{i,j=1}^{M}\sum_{n,m=1}^{L}\mathbb{E}\left\{\Re\{y_{\text{t}}^i(n)\}^2\Re\{y_{\text{t}}^j(m)\}^2 + \Re\{y_{\text{r}}^i(n)\}^2\Re\{y_{\text{r}}^j(m)\}^2 - 2\Re\{y_{\text{t}}^i(n)\}^2\Re\{y_{\text{r}}^j(m)\}^2\right\}$$
$$\overset{(a)}{\approx} \frac{1}{ML}\left\{\mathbb{E}[\Re\{y_{\text{t}}^i(n)\}^4] + \mathbb{E}[\Re\{y_{\text{r}}^i(n)\}^4] - 2\mathbb{E}[\Re\{y_{\text{t}}^i(n)\}^2]\mathbb{E}[\Re\{y_{\text{r}}^i(n)\}^2]\right\} \tag{11}$$
$$+ \frac{ML-1}{ML}\left\{\mathbb{E}\left[\Re\{y_{\text{t}}^i(n)\}^2\right] - \mathbb{E}\left[\Re\{y_{\text{r}}^i(n)\}^2\right]\right\}^2 = \frac{1}{ML}(\phi_{\text{t}} + \phi_{\text{r}} - 2\varphi_{\text{t}}\varphi_{\text{r}}) + \frac{ML-1}{ML}(\varphi_{\text{t}} - \varphi_{\text{r}})^2.$$

When quantization errors are negligible and $\frac{\sigma_{\text{s}}^2}{\sigma_{\text{n}}^2} \to 0$,

$$\lim_{e_{\text{t}}^i, e_{\text{r}}^i, \frac{\sigma_{\text{s}}^2}{\sigma_{\text{n}}^2}\to 0} \text{Var}(\rho_{\text{array}}) = \lim_{e_{\text{t}}^i, e_{\text{r}}^i, \frac{\sigma_{\text{s}}^2}{\sigma_{\text{n}}^2}\to 0} \text{Var}(\rho_{\text{array}}|\mathcal{E}) = \sigma_{\text{n}}^4/(ML_1) + \sigma_{\text{n}}^4/(ML_2). \tag{26}$$

With $L_1 + L_2 = 2L$, the minimum variance is achieved when

$$L_1 = L_2 = L. \tag{27}$$

This solution also applies to the single-dish RAS. Next, substituting (27) to (24), the approximated mean μ_ρ of the estimated astronomical source power is

$$\mu_\rho = \mathbb{E}[\mu_{\rho|\mathcal{E}}] \approx \sigma_{\text{s}}^2 \tag{28}$$

where the approximation is due to the assumption $\mathbb{E}\left[|e_{\text{t}}^i(n)|^2\right] = \mathbb{E}\left[|e_{\text{r}}^i(n)|^2\right]$ since $\sigma_{\text{s}}^2 \ll \sigma_{\text{n}}^2$. Substituting (27) to (25), we obtain the variance σ_{array}^2 of the estimated astronomical source power as in (29) shown at the top of the next page. The first approximation in (29) holds because

$$\text{Var}(\mathbb{E}[\rho_{\text{array}}|\mathcal{E}]) = \mathbb{E}\left[\sigma_{\text{s}}^2 + (\text{MSE}_{\text{t}}(L) - \text{MSE}_{\text{r}}(L))/(ML)\right]^2 - \sigma_{\text{s}}^4 \approx 0. \tag{30}$$

The second approximation in (29) is due to $\sigma_{\text{s}}^2 \ll \sigma_{\text{n}}^2$ and $\mathbb{E}\left[|e_{\text{t}}^i(n)|^2\right] \ll \sigma_{\text{n}}^2$.

Similarly, we can also obtain approximate results for the single-dish RAS. The mean value of the estimated source power is the same as (28) while the variance is

$$\sigma_{\text{single}}^2 \approx 2\sigma_{\text{n}}^4/N. \tag{31}$$

Note that the approximate closed-form results correspond to the scenario with very low SNR (relevant for RAS) and negligible quantization error. Thus, comparison between the exact expressions from the previous section and the approximate ones will reveal the effect of quantization errors on the RAS power estimation performance. To observe this, we define their ratios as the normalized performance metrics as

$$\gamma_\mu \triangleq \mathbb{E}[\rho_{\text{single}}]/\mu_\rho = \mathbb{E}[\rho_{\text{array}}]/\mu_\rho \tag{32}$$

$$\gamma_\sigma \triangleq \text{Var}(\rho_{\text{single}})/\sigma_{\text{single}}^2 = \text{Var}(\rho_{\text{array}})/\sigma_{\text{array}}^2. \tag{33}$$

We present the effect of ADC resolution on the RAS power estimation performance by plotting γ_μ and γ_σ under various ADC resolutions in Fig. 2 and Fig. 3 respectively, where we apply trained Lloyd-Max quantizers corresponding to the noise variance. To verify the analytical results, we conducted Monte Carlo simulations using $\sigma_s^2 = 1$ and $\text{SNR} = -20$ dB. TABLE I shows the corresponding simulation results which match with the analytical results in Fig. 2 and Fig. 3. From the results in the figures, the following observations are in order: 1) A smaller ADC resolution introduces a larger bias to the mean of the RAS power estimation. 2) To obtain approximately unbiased estimates without additional bias compensation, an ADC resolution of at least 6 bits is needed. 3) The variance of the RAS power estimation reduces with decreasing ADC resolution. 4) The effects of ADC resolution in terms of the estimation mean and variance are approximately constant within the typical SNR range of interest for RAS (< -20 dB). This also allows us to use a small ADC resolution (causing a bias) and then compensate the precomputed bias.

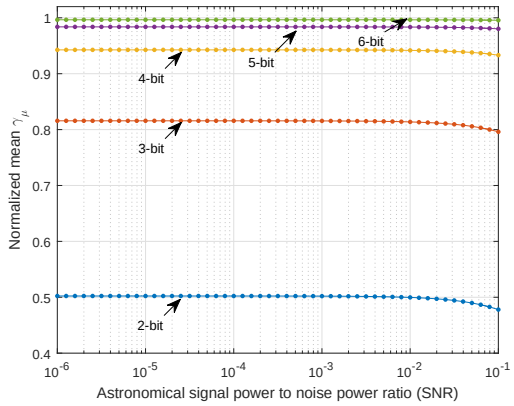

Fig. 2. Performance of normalized mean of RAS signal power estimation under various ADC resolutions ($\sigma_s^2 = 1$, N or $L = 10^4$)

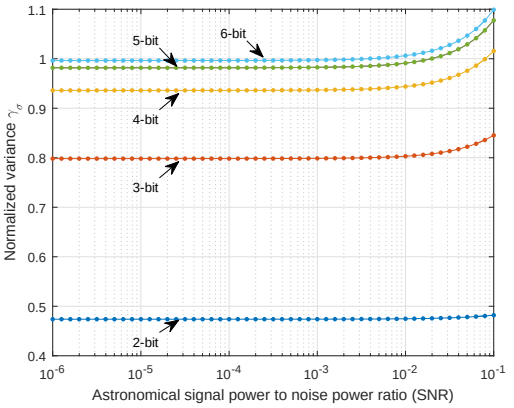

Fig. 3. Performance of normalized variance of RAS signal power estimation under various ADC resolutions ($\sigma_s^2 = 1$, N or $L = 10^4$)

After the bias compensation (i.e., multiplying with $1/\gamma_\mu$), the variance of the unbiased RAS power estimation is given by

$$\gamma_{\sigma,\text{unbiased}} \triangleq \frac{\text{Var}(\rho_{\text{single}}/\gamma_\mu)}{\sigma_{\text{single}}^2} = \frac{\text{Var}(\rho_{\text{array}}/\gamma_\mu)}{\sigma_{\text{array}}^2} = \frac{\gamma_\sigma}{\gamma_\mu^2}. \tag{34}$$

It is crucial for the RAS power estimator to be unbiased and

$$\sigma^2_{\text{array}} = \mathbb{E}\left[\text{Var}(\rho_{\text{array}}|\mathcal{E})\right] + \text{Var}(\mathbb{E}[\rho_{\text{array}}|\mathcal{E}])$$
$$\approx \frac{2}{ML}\sigma^4_{\text{n}} + \frac{1}{ML}(2\sigma^2_s\sigma^2_{\text{n}} + \sigma^4_{\text{s}}) + \frac{2}{ML}(\sigma^2_{\text{n}} + \sigma^2_{\text{s}})\mathbb{E}\left[|e^i_{\text{t}}(n)|^2\right] + \frac{2}{ML}\sigma^2_{\text{n}}\mathbb{E}\left[|e^i_{\text{r}}(n)|^2\right] \approx \frac{2\sigma^4_{\text{n}}}{ML}. \quad (29)$$

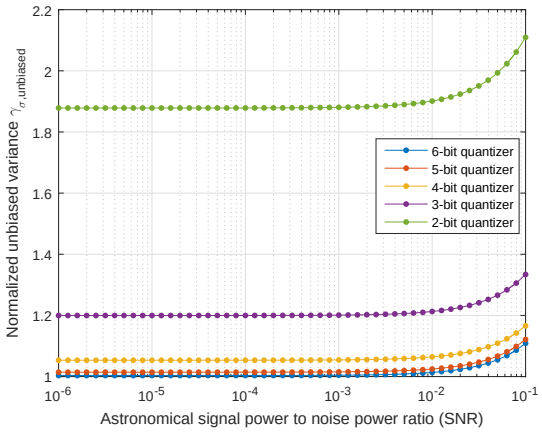

Fig. 4. Performance of normalized variance of RAS signal power estimation after the bias compensation ($\sigma^2_s = 1,\ N$ or $L = 10^4$)

hence, (34) is a more meaningful metric.

Fig. 4 presents the variance of the unbiased RAS power estimator for different ADC resolutions. We can observe that a higher ADC resolution yield a smaller variance. However, the performance saturates for ADC resolution of 6 bits or more. We also simulated 7 and 8 bits ADC resolutions and the results are indistinguishable from that of 6 bits ADC and hence they are not plotted in Fig. 4 for the sake of clarity of the other curves. And $\gamma_{\sigma,\text{unbiased}}$ converges to 1 as the resolution increases. As a larger ADC resolution yield a higher data rate, trade-offs can be made between data rates and estimation performance. A good choice is 6 bits ADC resolution as more bits do not yield noticeable performance improvement.

Next, we evaluate the effect of the number of antennas. With the settings that $\sigma^2_{\text{s}} = 1$ and $N = 10^4$, TABLE II shows the Monte Carlo simulation results for a 4-bit quantizer at $\text{SNR} = -20\text{dB}$ when the number of antenna elements varies. Comparing the multi-antenna results to the single antenna result in this table, we observe the following. 1) The variance of estimated power decreases by a factor around M when more antennas are combined. This illustrates a benefit of the DRT system. 2) The corresponding normalized metric γ_σ, which in its approximate form in (14) is independent of M, slightly increases with M. This is due to the mismatch between the assumption of independence among the received signals at different antennas in the analysis and the correlation of the received signals across antennas due to the same astronomical signal in the simulation. In other words, the difference between γ_σ for $M > 1$ and γ_σ for $M = 1$ implies how accurate the approximation in (14) is, and the results show good accuracy. 3) The simulation result of γ_μ does not grow with M (thus, maintaining unbiased estimation for different values of M) since the signal correlation does not affect the mean.

TABLE I
COMPARISON OF DIFFERENT QUANTIZATION RESOLUTIONS

Bits	2	3	4	5	6
Simulated Mean (or γ_μ)	0.4967	0.8106	0.9447	0.9746	0.9986
Simulated Variance	0.9528	1.6165	1.8896	1.9871	2.0089
Corresponding γ_σ	0.4764	0.8082	0.9448	0.9936	1.0044

TABLE II
COMPARISON OF DIFFERENT NUMBERS OF ANTENNA ELEMENTS

M	1	10	50
Simulated Mean (or γ_μ)	0.9447	0.9421	0.9402
Simulated Variance	1.8896	0.1896	0.0386
Corresponding γ_σ	0.9448	0.9481	0.9640

V. PERFORMANCE COMPARISON

Here, we evaluate the performance of the DRT by incorporating specifics of the coexistence paradigm and then compare it with the performance of the single-dish RAS (the isolation paradigm). Recall the system parameters for the shared spectrum access described in Section II. Suppose the hourly allocation of the number of subframes per frame to the three phases is pre-designed according to the CWC traffic statistics as in [10]. Let $n_{\text{array},l}$ denote the number of subframes per frame allocated to the DRTs for the lth hour. An example of available observation intervals of DRT in terms of $n_{\text{array},l}$ is shown by a line curve in Fig. 5 based on the system setting in [10]. DRT is allocated with longer (shorter) observation intervals during hours with lower (higher) CWC average traffic loads. Thus, the hourly estimation performance of DRT would vary as well.

The number of samples at hour l for DRT is given by $2L_l = 2Bn_{\text{array},l}T_{\text{sf}}N_{\text{f/hour}}$ while that for the single-dish RAS is $2N = 2Bn_{\text{f}}T_{\text{sf}}N_{\text{f/hour}}$ at any hour. Then, the variances of the estimated powers in (29) and (31) for hour l are

$$\sigma^2_{\text{array},l} \approx \frac{2\sigma^4_{\text{n}}}{MBn_{\text{array},l}T_{\text{sf}}N_{\text{f/hour}}}, \quad l = 1, \ldots, 24 \quad (35)$$

$$\sigma^2_{\text{single},l} = \frac{2\sigma^4_{\text{n}}}{Bn_{\text{f}}T_{\text{sf}}N_{\text{f/hour}}}, \quad l = 1, \ldots, 24. \quad (36)$$

As hourly based signal power estimates denoted by $\{\rho_{\text{array},l}\}$ have different accuracies, if the desired power estimation needs to be computed over K hours $(l_1, \ldots, l_K)$, we can apply the best linear unbiased estimation [19] to combine the K estimates as

$$\rho_{\text{array}} = \sum_{k=1}^{K} \rho_{\text{array},l_k} \frac{1/\sigma^2_{\text{array},l_k}}{\sum_{n=1}^{K} 1/\sigma^2_{\text{array},l_n}}. \quad (37)$$

The corresponding estimator variance for the DRT system is

$$\sigma^2_{\text{array}} \approx \frac{2\sigma^4_{\text{n}}}{MBT_{\text{sf}}N_{\text{f/hour}}\sum_{k=1}^{K} n_{\text{array},l_k}}. \quad (38)$$

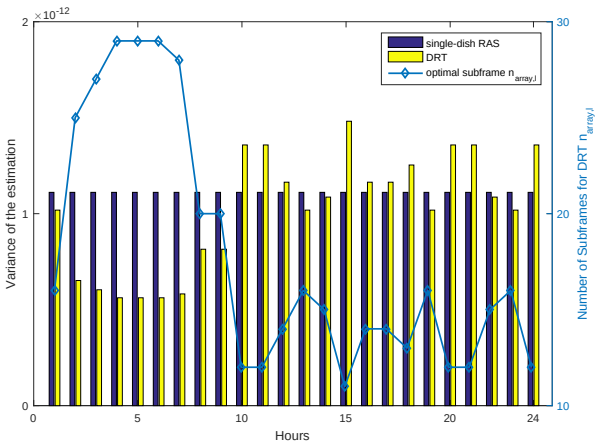

Fig. 5. Accuracy Performance Comparison and Optimal Subframe Numbers

For the single-dish RAS, we obtain the estimate as $\rho_{\text{single}} = \sum_{k=1}^{K} \rho_{\text{single},l_k}/K$ and the corresponding variance is

$$\sigma^2_{\text{single}} = \frac{2\sigma^4_{\text{n}}}{KBn_{\text{f}}T_{\text{sf}}N_{\text{f/hour}}}. \tag{39}$$

In a typical deployment of the shared spectrum access, a fixed minimum value of $n_{\text{CWC+RAS},l} = n_{\text{CWC+RAS}}$ would be used. Let β denote the ratio of the total resources allocated over the above K hours between CWC and RAS, i.e., $\beta = (\sum_{k=1}^{K} n_{\text{CWC},l_k})/(\sum_{k=1}^{K} n_{\text{RAS},l_k})$. Then, with $\eta \triangleq (n_{\text{f}} - n_{\text{CWC+RAS}})/n_{\text{f}}$, we have

$$\sum_{k=1}^{K} n_{\text{array},l_k} = \frac{\eta K}{1+\beta} n_{\text{f}}. \tag{40}$$

Next, from (38), (39) and (40), we obtain

$$\sigma^2_{\text{array}} \approx \frac{1+\beta}{M\eta}\sigma^2_{\text{single}}. \tag{41}$$

The above equation shows the relationship between the estimation accuracy of the DRT system and that of the single-dish RAS. For example, to achieve the same or better estimation performance than the single-dish RAS, the DRT system needs at least $M = \lceil \frac{1+\beta}{\eta} \rceil$ antenna elements.

To compare the estimation accuracy, we assume that $\sigma^2_{\text{n}} = 1$, $K = 24$, $B = 500$MHz, $T_{\text{sf}} = 38.5\mu s$, $n_{\text{f}} = 44$, $n_{\text{CWC+RAS}} = 4$, $\beta = 1.25$. Then, we have $M = \lceil \frac{1+\beta}{\eta} \rceil = 3$. Next, according to the $n_{\text{array},l}$ curve shown in Fig. 5, the variances of estimated power in each hour are computed and also presented in Fig. 5. Clearly, the variance of estimated power of the DRT system is inversely proportional to the number of allocated subframes while the single-dish RAS's variance remains a constant value. Combining all the estimates by the best linear unbiased estimation, we find the corresponding variances for the DRT system and the single-dish RAS are $\sigma^2_{\text{array}} = 3.82\times10^{-14}$ and $\sigma^2_{\text{single}} = 4.63\times10^{-14}$, respectively. Therefore, with enough numbers of DRTs, the DRT system can provide better estimation accuracy than the single-dish RAS.

VI. Conclusions

We have proposed a DRT system to embrace the geographical and spectral coexistence between CWC and RAS, and to enhance the capability or performance of RAS. Under the time-division based shared spectrum access, not only RFI-free spectrum access is available to DRT during pre-designed time slots, but also more DRTs can be deployed without requiring radio quiet zones. We have derived the theoretical performance analysis of the RAS signal power estimation under different ADC resolutions and their closed-form approximations for both the DRT system and the single-dish RAS with radio quiet zone. Different ADC resolutions introduce different biases to the RAS power estimation. With the bias compensation, the 6-bits ADC resolution offers a good tradeoff between the estimation variance and the data rate. By exploiting more DRTs, the proposed DRT system can perform as accurate as (or better than) the conventional single-dish RAS.

References

[1] *National Research Council, Spectrum management for science in the 21st century*. National Academies Press, 2010.

[2] ITU-R, *Protection creteria used for radio astronomical measurements*. ITU, Recommendation RA.769-2, Mar. 2003.

[3] *National Research Council, Handbook of Frequency Allocations and Spectrum Protection for Scientific Uses*. National Academies Press, 2007.

[4] W. Van Driel, "Radio quiet, please!–protecting radio astronomy from interference," *Proc. Intl. Astronomical Union*, vol. 5, no. S260, pp. 457–464, 2009.

[5] P. Pritzker and L. E. Strickling, "Fourth interim progress report on the ten-year plan and timetable and plan for quantitative assessments of spectrum usage," Tech. Rep., June 2014.

[6] Z.-Q. Luo and S. Zhang, "Dynamic spectrum management: Complexity and duality," *IEEE J. Sel. Topics in Signal Process.*, vol. 2, no. 1, pp. 57–73, 2008.

[7] R. Q. Hu and Y. Qian, "An energy efficient and spectrum efficient wireless heterogeneous network framework for 5G systems," *IEEE Commun. Mag.*, vol. 52, no. 5, pp. 94–101, 2014.

[8] Y. Liao, *et al.*, "Full duplex cognitive radio: a new design paradigm for enhancing spectrum usage," *IEEE Commun. Mag.*, vol. 53, no. 5, pp. 138–145, 2015.

[9] D. Emerson, "Why single-dish?" in *Single-Dish Radio Astronomy: Techniques and Applications*, vol. 278, 2002, pp. 27–43.

[10] H. Minn, Y. R. Ramadan, and Y. Dai, "A new shared spectrum access paradigm between cellular wireless communications and radio astronomy," in *IEEE GLOBECOM*, 2016, pp. 1–6.

[11] Y. R. Ramadan, H. Minn, and Y. Dai, "A new paradigm for spectrum sharing between cellular wireless communications and radio astronomy systems," *IEEE Trans. Commun.*, 2017, DOI: 10.1109/TCOMM.2017.2709319.

[12] Y. R. Ramadan, *et al.*, "Spectrum sharing between WiFi and radio astronomy," in *Radio Frequency Interference*. IEEE, 17-20 Oct. 2016.

[13] S. S. Bhattacharyya, *et al.*, *Handbook of signal processing systems*. Springer Science & Business Media, 2013.

[14] G. Hellbourg, *et al.*, "Statistical performance of reference antenna based spatial RFI mitigation for radio astronomy," in *IEEE Intl. Symp. Antennas and Propagation,* 2015, pp. 1518–1519.

[15] B. D. Jeffs, *et al.*, "Auxiliary antenna-assisted interference mitigation for radio astronomy arrays," *IEEE Trans. Signal Process.*, vol. 53, no. 2, pp. 439–451, 2005.

[16] A. M. Sardarabadi, *et al.*, "Spatial filtering of RF interference in radio astronomy using a reference antenna array," *IEEE Trans. Signal Process.*, vol. 64, no. 2, pp. 432–447, 2016.

[17] T. L. Wilson, *et al.*, *Tools of radio astronomy*, 6th ed. Springer, 2009.

[18] A. Colliander, *et al.*, "Noise injection radiometer test specifications and requirement," *Helsinki Univ. of Technology*, 2002.

[19] S. M. Kay, "Fundamentals of statistical signal processing, volume i: Estimation theory," 1993.